Journal of Physiology (1993), **460**, *pp.* 117–133
With 9 figures
Printed in Great Britain

Ca^{2+} AND Ca^{2+}-ACTIVATED Cl^- CURRENTS IN RABBIT OESOPHAGEAL SMOOTH MUSCLE

BY H. I. AKBARALI AND W. R. GILES*

From the Departments of Medical Physiology and Medicine, Faculty of Medicine, University of Calgary, 3330 Hospital Drive, N.W. Calgary, Alberta, Canada T2N 4N1

(*Received 19 December 1991*)

SUMMARY

1. An inward current carried by Ca^{2+} was recorded from single smooth muscle cells of rabbit oesophageal muscularis mucosae using a whole-cell gigaseal technique with physiological (2 mM) external calcium concentration ($[Ca^{2+}]_o$) in the presence of intracellular Cs^+ ($[Cs^+]_i$ 130 mM). Only one type of Ca^{2+} current could be identified. The threshold for its activation was approximately −30 mV and maximum inward current (approximately 300 pA) was recorded at 0 mV.

2. This inward current was blocked by Co^{2+} (4 mM), Cd^{2+} (0·5 mM) and nifedipine (1 μM) and was enhanced by Bay K 8644 (5 μM). We therefore classify it as a L-type Ca^{2+} current and denote it I_{Ca}.

3. Steady-state inactivation data were well-fitted by a Boltzmann distribution, indicating that inactivation of the Ca^{2+} current is strongly modulated by membrane potential. However, the inactivation of I_{Ca} slowed significantly and became less complete when $BaCl_2$ replaced $CaCl_2$ in the Tyrode solution suggesting that the inactivation of I_{Ca} may also be dependent on $[Ca^{2+}]_i$. The steady-state activation and inactivation curves for I_{Ca} overlap between −40 and 0 mV indicating that there may be a Ca^{2+} window current in this range of potentials.

4. When EGTA was omitted from the pipette-filling solution, depolarizations positive to −10 mV resulted in a transient as opposed to a maintained inward Ca^{2+} current which was followed by a relatively large outward current. Under these conditions, slowly decaying inward tail currents were also recorded upon repolarization to the holding potential, −60 mV. However, when EGTA was omitted from the pipette, marked 'run-down' of the Ca^{2+} current occurred within 10 min after starting the whole-cell recording.

5. This run-down of I_{Ca} was reduced significantly when the nystatin perforated patch technique was used. Under these conditions stable I_{Ca} records could be obtained for over 1 h. Outward currents and slow decaying inward tail currents similar to those recorded with no EGTA in the pipette were also obtained consistently using the nystatin recording technique.

6. In nystatin perforated patch recordings, $CoCl_2$ (2 mM) completely abolished the Ca^{2+} current, the outward currents and the slow inward tails. These findings suggest

* To whom correspondence should be addressed.

MS 9561

that the outward currents and slow inward tails are activated by a transmembrane influx of Ca^{2+}.

7. Ion replacement and pharmacological tests provided evidence that both the outward currents and the slow inward tails are due to Ca^{2+}-activated Cl^- current ($I_{Cl(Ca)}$). Thus, (i) the reversal potential of the tail currents was dependent on the electrochemical gradient for Cl^-, and (ii) the current onsets and tails were significantly reduced by niflumic acid (10 μM) and anthracene-9-carboxylic acid (9-AC; 300 μM). 4,4′-Diisothiocyanostilbene-2,2′-disulphonic acid (DIDS) and 4-acetamindo-4-isothiocyanostilbene-2,2′-disulphonic acid (SITS) also partially blocked these current changes.

8. Our results provide the first information on the biophysical properties of I_{Ca} and $I_{Cl(Ca)}$ in oesophageal smooth muscle. The data obtained using the nystatin technique demonstrate that I_{Ca} is physiologically important both as a source of electrogenic current and as an activator of other Ca^{2+}-dependent current systems, e.g. $I_{Cl(Ca)}$.

INTRODUCTION

The tunica muscularis mucosae (TMM) is an inner smooth muscle coat of the mammalian gastrointestinal tract. Both motoneurones and non-adrenergic, non-cholinergic nerves innervate the TMM via the surrounding intrinsic submucosal plexus (Kamikawa, Shimo & Uchida, 1982; Akbarali, Bieger & Triggle, 1986). Very little is known about the role of the muscularis mucosae in oesophageal motility (for review see Goyal & Paterson, 1989). However, a consistent hyperpolarization has been observed due to 'swallow-induced' peristalsis in the muscularis muscosae of the opossum (Sugarbaker, Rattan & Goyal, 1984). Previous studies have also shown that oesophageal TMM responds to a variety of pharmacological stimuli (Christensen & Percy, 1984; Hughes, 1955; Kamikawa, Fujinuma & Shimo, 1985; Bieger & Triggle, 1985). The regional gradients in neural and pharmacological responsiveness of the TMM (Bieger & Triggle, 1985; Akbarali *et al.* 1986) suggest a functional role of this tissue in oesophageal motility.

Ca^{2+} antagonists are known to reduce the frequency, amplitude and duration of the peristaltic wave in the oesophagus and have been used in the treatment of diffuse oesophageal spasm (see Lydtin & Trenkwalder, 1990). Contractile responses to isotonic potassium in the rat oesophageal muscularis mucosae are also blocked by dihydropyridine calcium channel antagonists (Akbarali, Bieger & Triggle, 1988). In combination, these results suggest that a functionally important calcium conductance is present in the smooth muscle of mammalian oesophagus. The initial goal of the experiments reported in this paper was to examine the characteristics of the calcium conductance in this smooth muscle.

In the majority of published records of calcium currents in smooth muscle, the patch pipette contains caesium and/or high concentrations of EGTA to block the relatively large outward potassium currents, and to prevent run-down of the calcium current, respectively (Klöckner & Isenberg, 1985; Katzka & Morad, 1989). Although these types of recordings have been utilized to advantage, a potential drawback is that the artificial intracellular calcium buffering may reduce or eliminate other calcium-activated currents in these preparations. We have tested this possibility by comparing results obtained with conventional gigaseal recordings with those

obtained using the nystatin perforated patch technique. Our results demonstrate the presence of large Ca^{2+} currents and activation of Ca^{2+}-activated Cl^- currents in the rabbit TMM.

Ca^{2+}-activated Cl^- currents have been demonstrated in vascular smooth muscle (Byrne & Large, 1987; Pacaud, Loirand, Lavie, Mironneau & Mirronneau, 1989). For example, these currents can be activated by noradrenaline following intracellular Ca^{2+} release (Amedee, Large & Wang, 1990). Pacaud *et al.* (1989) reported that dialysing portal vein cells with intracellular Cs^+ in the absence of intracellular EGTA, resulted in the appearance of a late outward current followed by long-lasting inward tail currents, and these current changes were shown to be due to Ca^{2+}-activated Cl^- current ($I_{Cl(Ca)}$). $I_{Cl(Ca)}$ has also been demonstrated in rabbit pelvic parasympathetic ganglia and the inner segments of photoreceptors (see Mayer, Owen & Barker, 1990 for review). These currents are characterized by slow activation, slowly decaying inward tail currents on repolarization, and sensitivity to Ca^{2+} channel blockers.

METHODS

Cell dispersion

New Zealand White rabbits (1·5–2·0 kg) were killed by cervical dislocation following sodium pentobarbitone anaesthesia. The oesophagus was excised and placed in a low-Ca^{2+} Tyrode solution containing 8 μM Ca^{2+}. The TMM was separated from the striated tunica propria as described previously for the rat oesophagus (Bieger & Triggle, 1985) and was then dissected free of fat and connective tissue. The epithelium was stripped away since preliminary experiments demonstrated that it was necessary to remove the epithelium in order to obtain an acceptable yield of viable single cells. Only the distal 3·5–5 cm of the TMM was used. This tissue was cut into small pieces and incubated at 35 °C in the low-Ca^{2+} Tyrode solution for 30 min. These pieces of tissue were then incubated in the low-Ca^{2+} Tyrode solution containing collagenase (0·25 mg/ml) and trypsin (0·5 mg/ml) for 30 min. Following this, the tissues were treated again with collagenase (0·25 mg/ml) plus bovine serum albumin (1 mg/ml) in the low-Ca^{2+} Tyrode solution for 20–30 min, and then they were transferred to an enzyme-free solution containing bovine serum albumin (1 mg/ml). Finally, the tissue was triturated gently with a wide-bore fire-polished pipette until single cells were released. An aliquot of the resulting cell suspension was transferred to the recording chamber on the stage of an inverted microscope (Nikon Diaphot, Tokyo, Japan). Smooth muscle cells were identified by their morphology (elongated, spindle-like shape).

Solutions

All experiments were carried out at room temperature (21–23 °C). The low-Ca^{2+} Tyrode solution had the following composition (mM): NaCl, 137; KCl, 2·7; $CaCl_2$, 0·008; $MgCl_2$, 0·88; NaH_2PO_4, 0·36; $NaHCO_3$, 12; glucose, 5·5. This solution was equilibrated with 95% O_2–5% CO_2. During electrophysiological recordings a HEPES-buffered solution was used. It consisted of (mM): NaCl 135; KCl, 5·4; NaH_2PO_4, 0·33; HEPES, 5; $MgCl_2$, 0·8; $CaCl_2$, 2; glucose, 5·5. This solution was equilibrated with 100% O_2 and its pH adjusted to 7·4 with NaOH (1 N). The recording pipettes were filled with (mM): caesium aspartate, 100; CsCl, 30; HEPES, 5; $MgCl_2$, 1. The pH of the solution was adjusted to 7·2 with CsOH. In the conventional whole-cell recordings, 2 mM ATP (disodium salt) and 5 mM EGTA were also added to the pipette solution. In some experiments the Cl^- concentration in the pipette was increased to 130 mM by replacing caesium aspartate with CsCl. Liquid junction potentials were estimated by replacing extracellular solution with the pipette solution and the voltage offset was measured using a 3 M KCl–agar bridge as a reference.

Collagenase was obtained from Yakult Corporation (Tokyo, Japan). All other reagents and drugs were purchased from Sigma Co. Ltd (St Louis, MO, USA),

Electrical recordings

The gigaseal patch-clamp technique was used in the whole-cell configuration (Hamill, Marty, Neher, Sakmann & Sigworth, 1981). The voltage-clamp amplifier was an Axopath 1D (Axon Instruments, USA). Microelectrodes (World Precision Instruments, CT, USA, 1·00 mm diameter)

were prepared on Flaming/Brown horizontal puller (Sutter Instruments Co., USA). The resistance of these filled patch pipettes was 3–5 megaohms (MΩ). Membrane potential and current were monitored on a storage oscilloscope (Hitachi, V-134, Tokyo, Japan) and stored on a microcomputer (Zenith, Z-386 SX) using an analog-to-digital conversion board (Data Translation, DT 2801-A) controlled by a custom-made acquisition and display software (Robinson & Giles, 1986). After each experiment, the stored records were sent to DEC VAX 11-750 for analyses. Pipette and cell capacitance were electronically compensated using the capacity compensation circuit of the Axopatch amplifier. Preliminary experiments in which the capacity transient was recorded at a fast time base confirmed that the readings obtained from this amplifier did not differ significantly from the integrated response of the capacity transient.

Perforated patch recordings using nystatin

In some experiments whole-cell recordings were obtained using the nystatin perforated patch method as described by Horn & Marty (1988). Nystatin (Sigma Chemical Co., St Louis, MO, USA) stock solution (5 mg/ml) was prepared in dimethyl sulphoxide and diluted 1:500 in the pipette solution to give a final concentration of 100 μg/ml. The nystatin solution was sonicated to ensure complete solubilization. To obtain gigaohm seals, the tip of the pipette was filled with normal pipette solution and then the shank was back-filled with the nystatin solution. After forming the seal (2–10 GΩ), the capacity transient in response to −10 mV pulses was monitored continuously. Within 5–15 min the capacitative transient increased to a steady level. The access resistance measured after 15 min had decreased to about 10–30 MΩ; thereafter it remained stable for approximately 1 h in acceptable experiments.

RESULTS

Calcium currents

In conventional whole-cell recordings with Cs^+ in the pipette inward currents were consistently observed when the cell was depolarized positive to approximately −30 mV (Fig. 1). To avoid 'run-down' of these inward currents, 5 mM EGTA was routinely added to the pipette solution. Figure 1 shows inward currents in response to depolarizations from a holding potential of −60 mV in a cell bathed in 2 mM $[Ca^{2+}]_o$. An averaged *I–V* relationship for eight cells is shown in Fig. 1*B*. The threshold for the activation of this current was near −30 mV and the maximum inward current was recorded between 0 and +10 mV. The apparent reversal potential was approximately +60 mV. The maximum amplitude of the inward current was −315 ± 17 pA and its time to peak averaged 28 ms at 0 mV at 23 °C. The inward current density was calculated to be 6·1 ± 1·6 μA/cm² in 2 mM $[Ca^{2+}]_o$. The filled circles in Fig. 1*B* show that in the presence of 4 mM $CoCl_2$ the inward current was blocked completely. The dihydropyridine calcium channel blocker nifedipine (1·0 μM) also completely abolished this inward current (Fig. 2*A*). Conversely, the calcium channel agonist Bay K 8644 (5 μM) markedly enhanced it (Fig. 2*B*). When the holding potential was made more negative (−80 mV), peak inward current was enhanced (−426 ± 12 pA at 0 mV; $n = 6$); however, the threshold for the inward current was still recorded at −30 mV and no hump was observed (data not shown) in the current–voltage relationship, suggesting that no low threshold T-type Ca^{2+} current was present (Bean, 1985). Taken together, these results indicate that the inward current in the TMM cell is due to Ca^{2+} influx through time- and voltage-dependent, L-type Ca^{2+} channels.

The results in Figs. 1 and 2*A* and *B* show that this Ca^{2+} current exhibited significant inactivation in 2 mM $[Ca^{2+}]_o$. Replacing the Ca^{2+} with 2 mM Ba^{2+} resulted in a much slower inactivation (Fig 2*C*) suggesting that current-dependent

inactivation is present in rabbit oesophageal TMM cells. In 10 mM Ba^{2+} the peak inward current at 0 mV increased significantly (approximately 3-fold) and the peak of the *I–V* curve was shifted to more positive potentials (+10 mV) (data not shown). Further evidence for a component of current-dependent inactivation was obtained

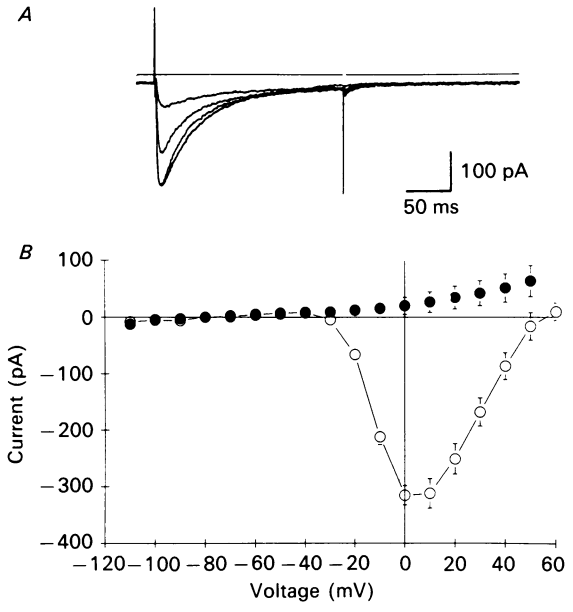

Fig. 1. Current–voltage relationship for inward Ca^{2+} current in TMM cells obtained using a conventional whole-cell recording technique. Depolarizing clamp steps were applied at 0·1 Hz for 200 ms from a holding potential of −60 mV. The superimposed family of inward currents shown in panel *A* was elicited by clamp steps to 0, +10, +20 and +30 mV. Panel *B* shows an averaged *I–V* curve from eight cells (○). ●, *I–V* curve obtained in the presence of 4 mM $CoCl_2$ (4 cells) which was used to block I_{Ca}. Data are shown as means±S.E.M. External solution, normal HEPES-buffered Tyrode solution containing 2 mM $CaCl_2$. The solution in the micropipette contained caesium aspartate (100 mM) with 5 mM EGTA.

using a double-pulse protocol (Fig. 2*D*). In these experiments, the Ca^{2+} current was activated by a depolarization from −70 to +10 mV (trace *a*, Fig. 2*D*); thereafter a prepulse to −10 mV was applied, which resulted in almost complete inactivation of the Ca^{2+} current (trace *b*, Fig. 2*D*). Next, a much more positive (+60 mV) prepulse was used (trace *c*, Fig. 2*D*) and paradoxically, the Ca^{2+} current recovered to approximately half the size of the control current. In combination, the data in Fig. 2 suggest that the Ca^{2+} current in this preparation obeys both time- and voltage-dependent as well as current-dependent inactivation.

Voltage-dependent inactivation of I_{Ca}

The voltage dependence of steady-state inactivation of I_{Ca} was studied in detail using a double-pulse protocol (Fig. 3). A variable conditioning pulse (P1) was applied for 2 s (not shown) immediately before a fixed test pulse (P2) to 0 mV. During P1 the

calcium current activated and then inactivated to a steady-state level at the P1 voltage; the subsequent P2 pulse activated only the remaining Ca^{2+} channels. For a conventional time- and voltage-dependent Hodgkin–Huxley conductance, the steady-state inactivation curve describes the relative number of available Ca^{2+}

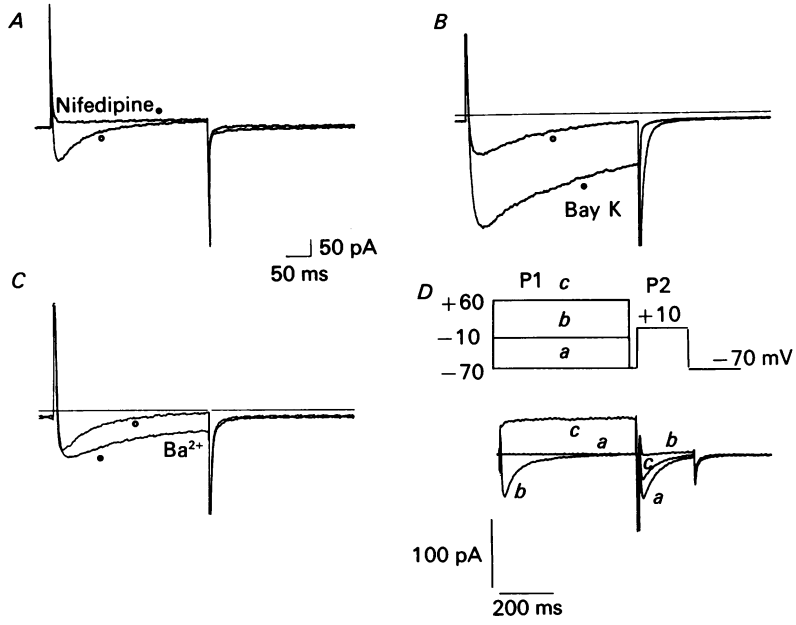

Fig. 2. Effects of 1 mM nifedipine (*A*), 5 mM Bay K 8644 (*B*), 2 mM $BaCl_2$ (*C*) and current-dependent inactivation of the Ca^{2+} current (*D*). *A–C*, I_{Ca} was elicited in three different cells by 200 ms pulses to test potentials of +10 mV from a holding potential of −60 mV, in the absence of (○) and presence (●) of the experimental compound. In *C*, $[Ca^{2+}]_o$ was replaced by Ba^{2+}. The solution in the recording pipette was the same as in Fig. 1. In *D* a conditioning prepulse (P1) was applied for 500 ms, followed by a 200 ms test pulse (P2) after a 10 ms gap to allow for settling of capacitative transient. Trace *a* shows Ca^{2+} current obtained in the absence of a conditioning prepulse. Trace *b* shows inactivation of the Ca^{2+} current after a prepulse (P1) to −10 mV. Note that in trace *c*, the Ca^{2+} current recovers after a prepulse to +60 mV.

channels (Fig. 3*B*) as a function of voltage. This sigmoidal curve can be described by a Boltzmann distribution of the form

$$y = 1 + \exp[(V + V_{0.5}/k)]^{-1}, \quad \text{(i)}$$

where $V_{0.5}$ is the voltage at which half the channels are inactivated, and k is the slope factor at this voltage. In 2 mM $[Ca^{2+}]_o$, $V_{0.5}$ was −30·4 mV and the slope factor was 6·3 mV. These results indicate that at the resting potential of the cell, approximately −50 mV, nearly 80% of the calcium channels are available for activation.

I_{Ca} deactivates very rapidly (approximately 10 ms), and as a result, the tail currents due to I_{Ca} are very difficult to separate from the capacitative transients. In these experiments it was not possible to study deactivation of the calcium current directly; and the voltage dependence of activation was calculated from peak

current–voltage relationship for I_{Ca} assuming a reversal potential of +60 mV. Peak conductance was normalized and plotted against the test potential. The sigmoidal curve was fitted by a Boltzmann function of the form

$$d = [1 + \exp(V - V_{0.5}/k_d)]^{-1}, \quad \text{(ii)}$$

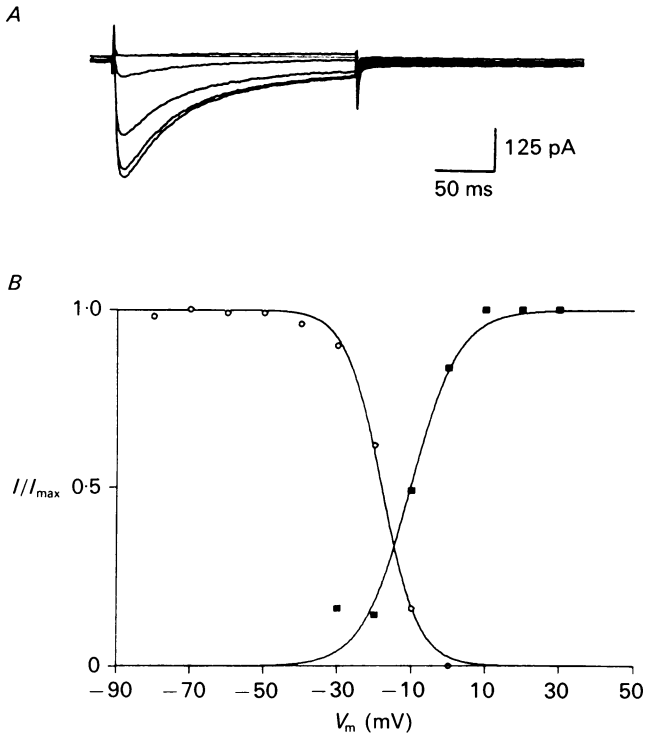

Fig. 3. Voltage-dependence of activation and inactivation of I_{Ca}. Panel *A* shows superimposed inward current records obtained after conditioning pulses to −70, −50, −30, −20, and 0 mV. The 2 s conditioning pulses (not shown) were followed immediately by a 200 ms test pulse to 0 mV. Panel *B*, inactivation (○) and activation (■) curves were fitted with Boltzmann functions. Note overlap of the two curves between −40 to 0 mV. See text for additional explanation and description.

where d is the activation parameter, $V_{0.5}$ was −17 mV, and the slope was 4·3 mV. Note that the activation and inactivation curves overlap between −40 and 0 mV, suggesting that there may be a 'window current' or non-inactivating I_{Ca}. The resulting Ca^{2+} current may be responsible for maintained Ca^{2+} influx during K^+-induced contractions (Akbarali *et al.* 1988; Imaizumi, Muraki, Takeda & Watanabe, 1989).

Cl^- currents

When the recording pipette contained 130 mM CsCl and EGTA was omitted, large depolarizations from a holding potential of −60 mV consistently elicited inward Ca^{2+} currents followed by substantial outward currents (Fig. 4). These outward

currents (which had complex kinetics) were observed at all potentials positive to +10 mV, and corresponding slow inward tail currents were recorded following repolarization to −60 mV when the Cl^- concentration in the pipette was 130 mM (reversal potential for Cl^-, $E_{Cl} = +3$ mV). In contrast, outward currents were

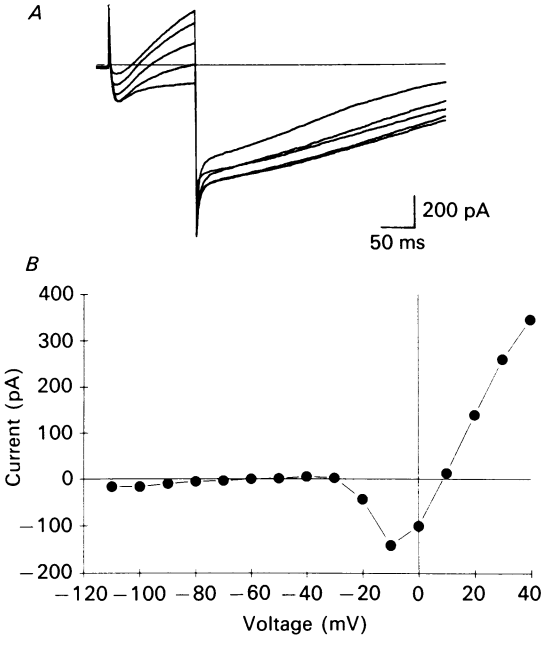

Fig. 4. Current records from a TMM cell obtained using conventional whole-cell recording technique with an internal solution containing 130 mM $CsCl_2$ and no EGTA. Panel *A*: holding potential, −60 mV; test potentials ranged from 0 to +40 mV in 10 mV steps. Panel *B* shows an isochronal *I–V* relationship of these currents measured at the end of the clamp steps.

activated at more negative voltages, approximately −30 mV in cells that were dialysed with 30 mM $[Cl^-]_i$ ($E_{Cl} = -36$ mV) (see Fig. 6) suggesting that the outward current(s) and the corresponding tails are carried by Cl^-.

Perforated patch recordings of I_{Ca}

Recordings made in the absence of EGTA exhibited significant 'run-down', usually within 5 min of beginning whole-cell recording. To overcome this problem, the nystatin perforated patch technique (Horn & Marty, 1988) was used. The results in Fig. 5*A* show that with the perforated patch technique large depolarizations evoked current changes that were very similar to those observed with conventional recordings in the absence of EGTA. These currents, however, could be maintained for a period of over 60 min without significant run-down. The threshold for their activation was near −20 mV and peak inward currents were recorded between −10 and 0 mV (Fig. 5*A* and *B*). With 30 mM $[Cl^-]_i$, outward currents were recorded at potentials positive to −30 mV and, on repolarization, slow inward tail currents were observed.

The dependence of these currents on transmembrane Ca^{2+} influx was examined by applying Co^{2+} (2 mM). As shown in Fig. 5*C*, the Ca^{2+} currents, the outward currents and the tail currents were completely abolished in the presence of Co^{2+}. The *I–V* relationship in Fig. 5*D* indicates that in the presence of Co^{2+}, outward currents could

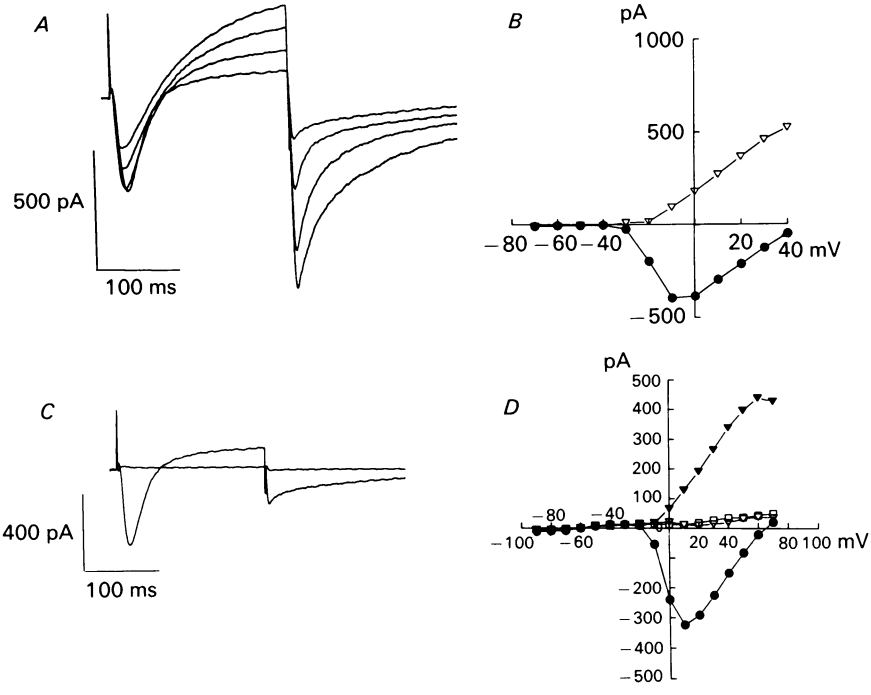

Fig. 5. Nystatin perforated patch recordings of Ca^{2+} and Ca^{2+}-activated outward currents. The patch pipette contained a caesium aspartate solution with nystatin (100 μg/ml). *A* shows recordings from a TMM cell held at −60 mV and depolarized to 0, +10, +20 and +30 mV. Following the Ca^{2+} currents, an outward current developed and on repolarization to −60 mV slow inward tail currents were recorded. *B* shows an *I–V* relationship for this Ca^{2+} current (●) and the outward current measured at the end of pulse (▽). In *C*, the current on depolarization to 0 mV is shown before and after 2 mM Co^{2+}. Note that all currents were blocked completely by Co^{2+}. *D* shows the *I–V* relationship for the Ca^{2+} currents (circles) and the outward current measured at the end of pulse (triangles). Closed symbols represent control currents and open symbols denote currents recorded in the presence of Co^{2+} (2 mM).

not be elicited even at very positive potentials (e.g. +70 mV). These results demonstrate that the outward current and the corresponding inward tails are dependent on transmembrane Ca^{2+} influx. The tail currents were also abolished when Ba^{2+} (10 mM) was used to replace Ca^{2+} as the charge carrier for the inward current (Fig. 6), and whenever the pipette contained high EGTA.

Somewhat similar large inward tail currents have been observed in other nerve and smooth muscle preparations. On the basis of ion replacement and blocker experiments, they have been attributed to chloride fluxes (Pacaud *et al.* 1989; Akasu, Nishimura & Tokimasa, 1990). Inward tail currents following an influx of Ca^{2+} can

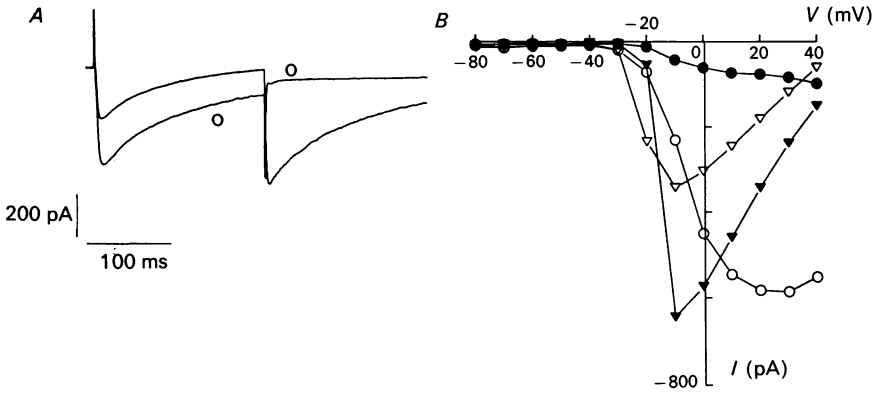

Fig. 6. Block of inward tail currents by $BaCl_2$. *A* shows currents recorded in the presence of 2 mM $[Ca^{2+}]_o$ and following replacement of $[Ca^{2+}]_o$ with 10 mM $[Ba^{2+}]_o$ (○) in perforated patch recordings from a TMM cell. The cell was depolarized from a holding potential of −60 mV to +10 mV for 200 ms. In the presence of $[Ba^{2+}]_o$, slow inward tail currents were markedly reduced. *B* shows current–voltage relationship obtained in the presence of Ca^{2+} (open symbols) and following replacement with Ba^{2+} (closed symbols). Triangles represent peak inward currents and circles denote amplitudes of tail currents.

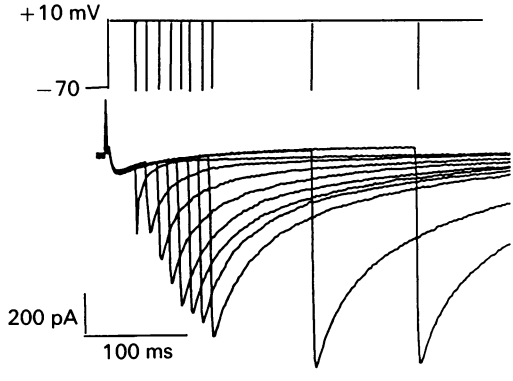

Fig. 7. Envelope of slow inward tail currents in rabbit oesophageal TMM cell. The cell was depolarized from −70 to +10 mV for durations ranging from 20 to 300 ms. After returning to −70 mV, an inward tail current was observed which increased as a function of the duration of the depolarization.

also be generated by the electrogenic Na^+–Ca^{2+} exchanger (Giles & Shimoni, 1989, cf. Wier, 1990). However, in TMM cells, replacement of Na^+ with TEA did not significantly alter the amplitude of the outward current or the inward tail currents, demonstrating that the Na^+–Ca^{2+} exchanger was not responsible for them.

The dependence of the inward tail currents on $[Ca^{2+}]_o$ was further examined by increasing the duration of depolarizing pulses. It would be expected that increasing the duration of the pulse would result in an increase in the amount of Ca^{2+} entering the cell and therefore would increase in intracellular Ca^{2+} levels. Figure 7 illustrates results from an experiment in which the duration of the depolarization pulse was increased from 20 ms to 300 ms. The envelope of tail shows a progressive increase in

the amplitude of the inward tail currents as the duration of the pulse is increased. Maximum inward tail current was observed at approximately 100 ms. Note that following short depolarizing pulses, the rate of decay of the inward tails was faster than during long pulses, suggesting that their deactivation may be modulated by $[Ca^{2+}]_i$ (Mayer *et al.* 1990).

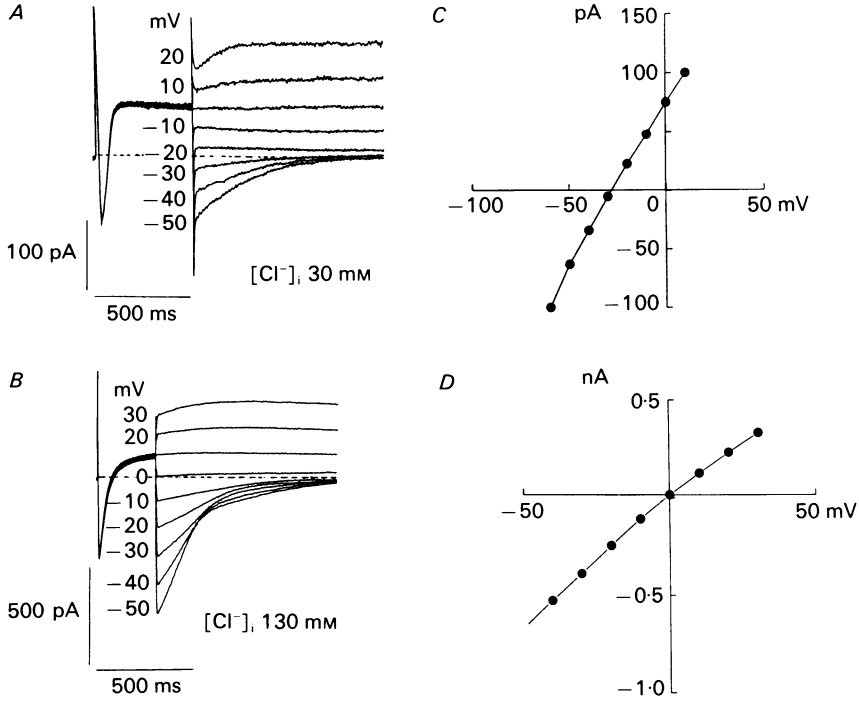

Fig. 8. Reversal of tail currents in rabbit TMM cells. Panels *A* and *C* show responses in a cell dialysed with 30 mM $[Cl^-]_i$. A conditioning pulse was applied to 0 from −60 mV for 200 ms; the membrane potential was then stepped back between −50 to +20 mV. Amplitude of the tails was measured 10 ms after repolarization to allow capacity transient to settle. Zero current level is indicated by dashed line. The plot of amplitude of tail current *vs.* membrane potential is shown on the right, demonstrating a reversal potential near −30 mV ($E_{Cl} = -36$ mV). Panel *B* shows responses obtained in another cell dialysed with 130 mM Cl^-. The conditioning pulse was applied from −60 to +10 mV for 100 ms. Under these conditions the tail current reversed near 0 mV (Panel *D*).

Chloride substitution

To obtain information concerning the ion selectivity of these outward currents, reversal potential measurements were made. Figure 8*A* shows that the tail currents recorded when the cell was dialysed with 30 mM $[Cl^-]_i$ reversed near −28 mV ($E_{Cl} = -36$ mV). The junction potential was about 10 mV when the $[Cl^-]_i$ was 30 mM. Figure 8*B* shows results from another cell in which 130 mM $[Cl^-]_i$ was present in the patch pipette. The tail currents in this case reversed near 0 mV, very close to the predicted E_{Cl} approximately 2 mV (Fig. 8*D*). These results suggest that this outward current is carried mainly by Cl^-.

Cl^- channel blockers

Further evidence that the outward current was generated by a Cl^- influx was obtained using a number of Cl^- channel blockers. The stilbene derivatives 4,4′-diisothiocyanatostilbene-2,2′-disulphonic acid (DIDS) and 4-acetamido-4′-isothiocyanatostilbene-2,2′-disulphonic acid (SITS) decreased both the Ca^{2+} currents and

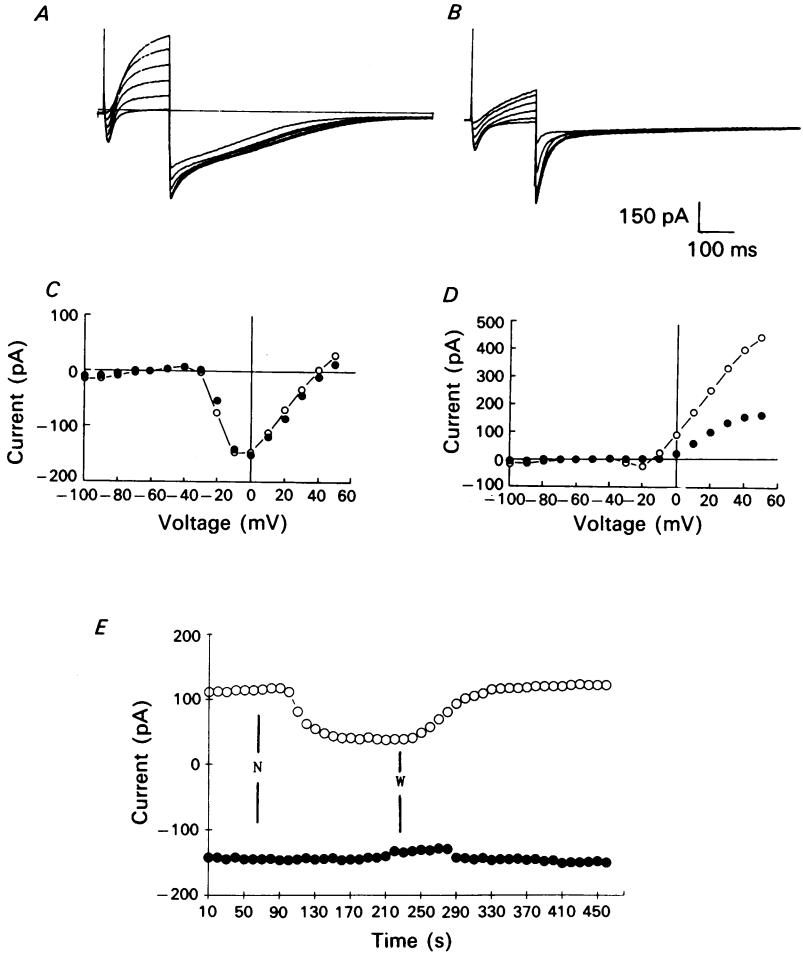

Fig. 9. Ca^{2+} currents recorded using the nystatin perforated patch technique. Families of superimposed currents in the absence (*A*) and presence (*B*) of 10 μM niflumic acid are shown. Test pulses from −10 to +40 mV were applied in 10 mV increments from the holding potential, −60 mV. Inward Ca^{2+} currents were followed by outward currents and slowly decaying tail currents (*A*) were observed on repolarization. Note that both the outward currents and inward tail currents were reduced by niflumic acid (*B*). Bottom panels show the *I–V* relationships for peak inward Ca^{2+} currents (*C*) and the current at the end of the pulse (*D*) in the absence (○) and presence (●) of niflumic acid. Panel *E* shows the time course of the effect of niflumic acid on outward and inward currents recorded using the perforated patch technique. Niflumic acid (10 μM) (N) decreased outward current (●) but did not affect inward current (○), and this inhibitory effect on outward Cl^- current was reversible on wash-out (W).

the Cl^- currents, making it impossible to interpret their effects unambiguously, since a partial block of the Ca^{2+} influx will result in a reduction of this Ca^{2+}-activated Cl^- current. Moreover, the inhibitory effects of DIDS and SITS persisted for over 30 min after wash-out. Similar results were obtained with Zn^{2+} (100 μM, $n = 3$). Previously, White & Aylwin (1990) described a reversible inhibition of Ca^{2+}-activated Cl^- currents in *Xenopus* oocytes by niflumic acid, a non-steroidal anti-inflammatory agent. In those experiments, both the outward current and the inward tails were reduced markedly by niflumic acid (10 μM) at concentrations which had no effect on Ca^{2+} current. Figure 9(*A–D*) shows that the outward currents were selectively reduced by niflumic acid, and Fig. 9*E* shows the time course of the effect of niflumic acid (10 μM) on the calcium currents and outward Cl^- currents. There was no significant change in I_{Ca}, but outward currents were reduced within 1 min and this effect was almost completely reversible. Higher concentrations of niflumic acid (100 μM) did not result in complete block of the outward or tail currents. Antracene-9-carboxylic acid (9-AC; 300 μM) also resulted in decrease in the amplitude of tail currents without significant effect on Ca^{2+} currents ($n = 4$, results not shown).

DISCUSSION

Our results describe some important properties of the Ca^{2+} current, and identify a Ca^{2+}-activated Cl^- current in single cells from the rabbit TMM. In addition, these data illustrate important differences in the pattern of results obtained with conventional whole-cell recordings, compared with the nystatin perforated patch method.

Ca^{2+} channels

The Ca^{2+} current density in the TMM (6·1 μA/cm^2) is similar to that in the intestinal smooth muscle (6·3 μA/cm^2; Ohya, Terada, Kitamura & Kuriyama, 1986) but is considerably smaller than that in guinea-pig taenia coli (19·5 μA/cm^2; Yamamoto, Hu & Kao, 1989) or urinary bladder (20 μA/cm^2; Klöckner & Isenberg, 1985). The Ca^{2+} current which we have identified in the TMM can be classified as L-type. The evidence for this includes (i) that the threshold for activation of I_{Ca} did not change when the holding potential was made more negative (−80 mV) and (ii) that I_{Ca} was blocked by nifedipine and enhanced by Bay K 8644 (Fig. 2). Previously, two types of Ca^{2+} channels have been shown to co-exist in a variety of vascular and non-vascular smooth muscle cells. In general, these have been separated based on their kinetics of activation and/or pharmacological responses (cf. Wong, 1991 for review; but also see Aaronson, Bolton, Lang & MacKenzie, 1988). At present, our results do not allow us to rule out the presence of another type of Ca^{2+} channel in the TMM since no single-channel analyses were carried out. Further studies using a combination of single-channel and whole-cell recordings will be required.

Our data show that I_{Ca} in the TMM shares many properties with I_{Ca} of other gastrointestinal smooth muscle cells, including both time- and voltage-dependent and current-dependent inactivation (guinea-pig taenia caeci: Ganitkevich, Shuba & Smirnov, 1987; rabbit intestinal smooth muscle: Ohya *et al.* 1986; canine colonic

myocytes: Langton, Burke & Sanders, 1989). These findings contrast with data from the ureter in which the mechanism of inactivation apparently can be described using only conventional time- and voltage-dependent formulations (Lang, 1990). In our experiments relatively large Ca^{2+} currents could be recorded in 2 mM $[Ca^{2+}]_o$, therefore the inactivation of I_{Ca} could be studied under conditions which are relevant to normal cellular function. The presence of a Ca^{2+} window current (Fig. 3) suggests that a non-inactivating I_{Ca} is present in TMM at potentials between −40 and 0 mV. This Ca^{2+} influx may account for maintained tonic contraction induced by high-K^+ solutions (Imaizumi *et al.* 1989).

Ca^{2+}-activated Cl^- currents

The Ca^{2+}-activated Cl^- current ($I_{Cl(Ca)}$), which we have identified is similar to the $I_{Cl(Ca)}$ which has been described previously in vascular smooth muscles (Byrne & Large, 1987; Pacaud *et al.* 1989). In cells from the rabbit ear artery, $I_{Cl(Ca)}$ was recorded in response to noradrenaline-induced $[Ca^{2+}]_i$ release (Amedee *et al.* 1990). In rat portal vein, Pacaud *et al.* (1989) recorded $I_{Cl(Ca)}$ in the absence of EGTA in the patch pipette. However, in our experiments, the absence of EGTA resulted in marked 'run-down' of the Ca^{2+} current. In contrast, the nystatin perforated patch method made it possible to record I_{Ca} and $I_{Cl(Ca)}$ which were both well maintained. It was therefore feasible to examine the properties of $I_{Cl(Ca)}$ in some detail.

The slow tail currents, which can be recorded when K^+ currents are blocked, are due to a Cl^- conductance since (1) the reversal potential changes as expected from the Nernst relationship when the $[Cl^-]_i$ is altered and (2) niflumic acid reduces this current. Our results show that DIDS is not selective for these Cl^- channels. These results are consistent with those of Amedee *et al.* (1990) who showed DIDs was more effective in blocking the cation conductance than the Cl^- channel in the rabbit ear artery. Niflumic acid has been shown to be an effective blocker of the Ca^{2+}-activated Cl^- channel in *Xenopus* oocytes (White & Aylwin, 1990) and in the rat portal vein (Pacaud *et al.* 1989). Our results confirm this by showing that at 10 μM niflumic acid substantially reduces the outward currents without affecting the Ca^{2+} currents. The activation of $I_{Cl(Ca)}$ in the TMM appears to be similar to other Ca^{2+}-activated Cl^- conductances, e.g. those described in cultured dorsal root ganglion neurones (Mayer, 1985) and in rabbit sympathetic ganglia (Akasu *et al.* 1990). In these preparations, Ba^{2+} failed to activate this Cl^- current. On the other hand, Scott, McGuirk & Dolphin (1988) reported that Ba^{2+} could induce the release of $[Ca^{2+}]_i$ and thereby indirectly activate $I_{Cl(Ca)}$. We have not examined the effects of $[Ca^{2+}]_i$ release on $I_{Cl(Ca)}$ in detail. However, Ba^{2+} which is known to release Ca^{2+} from intracellular stores in smooth muscle (Satoh, Kubota, Itoh & Kuriyama, 1987) failed to elicit either an outward current or inward tail currents in the rabbit TMM.

Ca^{2+}-dependent ionic currents in TMM

The results in this paper and our previous data (Akbarali, Giles & Nakajima, 1990) demonstrate that in the rabbit TMM at least two calcium-dependent currents can be observed, $I_{K(Ca)}$ and $I_{Cl(Ca)}$. Activation of $I_{Cl(Ca)}$ by neurohumoral agents could lead to depolarization since E_{Cl} is more positive than the resting membrane potential (Aickin, 1990). Conversely, $I_{Cl(Ca)}$ could also contribute to an after-hyperpolarization

following an action potential (Nishimura, Akasu & Tokimasa, 1991) or change the duration of the action potential and consequently after Ca^{2+} influx (Korn, Bolden & Horn, 1991).

In lacrimal gland cells, Marty, Tan & Trautmann (1984) reported that $I_{K(Ca)}$ was more sensitive than $I_{Cl(Ca)}$ to increases in $[Ca^{2+}]_i$. Experiments by Pacaud *et al.* (1989) also show that when the $[Ca^{2+}]_i$ was fixed at 0·5 μM, several depolarizing pulses were required to activate inward tail currents due to $I_{Cl(Ca)}$. These results suggest that $[Ca^{2+}]_i$ can modulate the size and kinetics of $I_{Cl(Ca)}$. In accordance with this, in TMM cells brief depolarizing pulses or large depolarizations to very positive potentials, both of which result in relatively small Ca^{2+} entry are followed by small inward tail currents which decay quite rapidly (Figs 6, 7 and 8).

Specification of the physiological role of the Ca^{2+}-activated Cl^- current in the TMM cells will require further investigation. Since 'off' depolarizations following neurally evoked hyperpolarization in the opossum oesophageal smooth muscle are abolished in Cl^--free medium (Daniel, Helmy-Elkholy, Jager & Kannan, 1983), the non-cholinergic non-adrenergic neurohumoral mediator (Akbarali *et al.* 1986) for these events may act by increasing a Cl^- conductance. Recent studies in opossum oesophageal circular muscle indicate that inhibitory junction potentials in response to single pulse stimulation may be mediated by a decrease in chloride conductance (Crist, He & Goyal, 1991).

In conclusion, our work provides new data concerning the electrophysiological properties of oesophageal TMM. Taken together with previous pharmacological data (see Akbarali *et al.* 1986) these results support the hypothesis that this muscle may contribute to oesophageal peristalsis, particularly in those species which lack smooth muscle propria, e.g. rabbit, rat, guinea-pig, dog (Inglefinger, 1958). The modulation of these ionic currents by neurohumoral agents in this smooth muscle is an important topic for further investigation.

This work was supported by the Alberta Heritage Foundation for Medical Research (AHFMR) and Medical Research Council of Canada. Dr Giles is an Alberta Heritage Foundation Medical Scientist and Dr Akbarali is a postdoctoral fellow of the Heart and Stroke Foundation of Canada and AHFMR.

REFERENCES

AARONSON, P. I., BOLTON, T. B., LANG, R. J. & MACKENZIE, I. (1988). Calcium currents in single isolated smooth muscle cells from rabbit ear artery in normal-calcium and high-barium solutions. *Journal of Physiology* **405**, 57–75.

AICKIN, C. C. (1990). Chloride transport across the sarcolemma of vertebrate smooth and skeletal muscle. In *Chloride Channels and Carriers in Nerve, Muscle and Glial Cells*, ed. ALVAREZ-LEEFMANS, F. J. & RUSSELL, J. M., pp. 209–249. Plenum Press, New York and London.

AKASU, T., NISHIMURA, T & TOKIMASI, T. (1990). Calcium-dependent chloride current in neurones of the rabbit pelvic parasympathetic ganglia. *Journal of Physiology* **422**, 303–320.

AKBARALI, H. I., BIEGER, D. & TRIGGLE, C. R. (1986). Tetrodotoxin-sensitive and insensitive relaxations in the rat oesophageal tunica muscularis mucosae. *Journal of Physiology* **381**, 49–63.

AKBARALI, H. I., BIEGER, D. & TRIGGLE, C. R. (1988). Inhibition of field stimulation-evoked relaxations in rat oesophageal smooth muscle by the calcium antagonist PN 200-110. *British Journal of Pharmacology* **95**, 512–518.

AKBARALI, H. & GILES, W. (1991). Ca^{2+} activated Cl^- currents in rabbit oesophageal smooth muscle. *Biophysical Journal* **59**, 263*a*.

AKBARALI, H. I., GILES, W. R. & NAKAJIMA, T. (1990). K^+ currents in rabbit single oesophageal tunica muscularis mucosae cells. *Journal of Physiology* **422**, 43*P*.

AMEDEE, T., LARGE, W. A. & WANG, Q. (1990). Characteristics of chloride currents activated by noradrenaline in rabbit ear artery cells. *Journal of Physiology* **428**, 501–506.

BEAN, B. P. (1985). Two kinds of calcium channels in canine atrial cells. Differences in kinetics, selectivity, and pharmacology. *Journal of General Physiology* **86**, 1–30.

BIEGER, D. & TRIGGLE, C. R. (1985). Pharmacological properties of mechanical responses of the rat oesophageal tunica muscularis mucosae. *British Journal of Pharmacology* **84**, 93–106.

BYRNE, N. G. & LARGE, W. A. (1987). Action of noradrenaline on single smooth muscle cells freshly dispersed from the rat anococcygeus muscle. *Journal of Physiology* **389**, 513–525.

CHRISTENSEN, J. & PERCY, W. H. (1984). A pharmacological study of oesophageal muscularis mucosae from cat, dog and American opossum (*Didelphis virginiana*). *British Journal of Pharmacology* **83**, 329–336.

CRIST, J. R., HE, X. D. & GOYAL, R. K. Chloride-mediated inhibitory junction potentials in opossum esophageal smooth muscle. *American Journal of Physiology* **261**, G752–762.

DANIEL, E. E., HELMY-ELKHOLY, A., JAGER, L. P. & KANNAN, M. S. (1983). Neither a purine nor VIP is the mediator of inhibitory nerves of opossum oesophageal smooth muscle. *Journal of Physiology* **336**, 243–260.

GANITKEVICH, V. YA., SHUBA, M. F. & SMIRNOV, S. V. (1987). Calcium-dependent inactivation of potential-dependent calcium inward current in an isolated guinea-pig smooth muscle cell. *Journal of Physiology* **392**, 431–449.

GILES, W. & SHIMONI, Y. (1989). Slow inward tail currents in rabbit cardiac cells. *Journal of Physiology* **417**, 447–463.

GOYAL, R. K. & PATERSON, W. G. (1989). Esophageal motility. In *Handbook of Physiology. The Gastrointestinal System. Motility and Circulation*, ed SCHULTZ, S. G. & WOOD, J. D., pp. 865–908. American Physiological Society, Bethesda, MD, USA.

HAMILL, O. P., MARTY, A., NEHER, E., SAKMANN, B. & SIGWORTH, F. J. (1981). Improved patch-clamp techniques for high-resolution current recording from cells and cell-free membrane patches., *Pflügers Archiv* **391**, 85–100.

HORN, R. & MARTY, A. (1988). Muscarinic activation of ionic currents measured by a new whole-cell recording method. *Journal of General Physiology* **92**, 145–159.

HUGHES, F. B. (1955). The muscularis mucosae of the oesophagus of the cat, rabbit and rat. *Journal of Physiology* **130**, 123–130.

IMAIZUMI, T., MURAKI, K., TAKEDA, M. & WATANABE, M. (1989). Measurement and stimulation of noninactivating Ca^{2+} current in smooth muscle cells. *American Journal of Physiology* **256**, C880–885.

INGELFINGER, F. J. (1958). Esophageal motility. *Physiological Reviews* **38**, 533–584.

KAMIKAWA, Y., FUJINUMA, S. & SHIMO, Y. (1985). Contractile responses of the guinea pig oesophageal muscularis mucosae in vitro to arachidonic acid and its metabolite. *European Journal of Pharmacology* **114**, 53–59.

KAMIKAWA, Y., SHIMO, Y. & UCHIDA, K. (1982). Inhibitory actions of catecholamines on electrically induced contractions of the submucous plexus longitudinal muscularis mucosae preparation of the guinea-pig oesophagus. *British Journal of Pharmacology* **76**, 271–277.

KATZKA, D. A. & MORAD, M. (1989). Properties of calcium channels in guinea-pig gastric myocytes. *Journal of Physiology* **413**, 175–197.

KLÖCKNER, U. & ISENBERG, G. (1985). Action potentials and net membrane currents of isolated smooth muscle cells. *Pflügers Archiv* **405**, 329–339.

KORN, S. J., BOLDEN, A. & HORN, R. (1991). Control of action potentials and Ca^{2+} influx by the Ca^{2+}-dependent chloride current in mouse pituitary cells. *Journal of Physiology* **439**, 423–437.

LANG, R. J. (1990). The whole-cell Ca^{2+} channel current in single smooth muscle cells of the guinea-pig ureter. *Journal of Physiology* **423**, 453–473.

LANGTON, P. D., BURKE, E. & SANDERS, K. M. (1989). Participation of Ca currents in colonic electrical activity. *American Journal of Physiology* **257**, C451–460.

LYDTIN, H. & TRENKWALDER, P. (1990). *Calcium Antagonists. A Critical Review*. Springer-Verlag, Berlin, Heidelberg, New York.

MARTY, A., TAN, P. & TRAUTMANN, A. (1984). Three types of calcium-dependent channel in rat lacrimal glands. *Journal of Physiology* **357**, 293–325.

MAYER, M. L. (1985). A calcium-activated chloride current generates the after-depolarization of rat sensory neurones in culture. *Journal of Physiology* **364**, 217–239.

MAYER, M. L., OWEN, D. G. & BARKER, J. L. (1990). Calcium-dependent chloride currents in vertebrate central neurones. In *Chloride Channels and Carriers in Nerve, Muscle and Glial Cells*, ed. ALVAREZ-LEEFMANS, F. J. & RUSSELL, J. M., pp. 355–364. Plenum Press, New York and London.

NISHIMURA, T., AKASU, T. & TOKIMASA, T. (1991). A slow calcium-dependent chloride current in rhythmic hyperpolarization in neurones of the rabbit vesicle pelvic ganglia. *Journal of Physiology* **437**, 673–690.

OHYA, Y., TERADA, K., KITAMURA, K. & KURIYAMA, H. (1986). Membrane currents recorded from a fragment of rabbit intestinal smooth muscle cell. *American Journal of Physiology* **251**, C335–346.

PACAUD, P., LOIRAND, G., LAVIE, J. L., MIRONNEAU, C. & MIRONNEAU, J. (1989). Calcium activated chloride current in rat vascular smooth muscle cells in short term primary culture. *Pflügers Archiv* **413**, 629–636.

ROBINSON, K. & GILES, W. R. (1986). A data acquisition, display and plotting program for the IBM PC. *Computer Programs in Biomedicine* **23**, 319–327.

SATOH, S., KUBOTA, Y., ITOH, T. & KURIYAMA, H. (1987). Mechanisms of the Ba^{2+}-induced contraction in smooth muscle cells of the rabbit mesenteric artery. *Journal of General Physiology* **89**, 215–237.

SCOTT, R. H., MCGUIRK, S. M. & DOLPHIN, A. C. (1988). Modulation of divalent cation-activated chloride ion currents. *British Journal of Pharmacology* **94**, 653–662.

SUGARBAKER, D. J., RATTAN, S. & GOYAL, R. K. (1984). Mechanical and electrical activity of esophageal smooth muscle during peristalsis. *American Journal of Physiology* **246**, G145–150.

WIER, W. G. (1990). Cytoplasmic calcium in mammalian ventricle: dynamic control by cellular processes. *Annual Review of Physiology* **52**, 467–485.

WHITE, M. M. & AYLWIN, M. (1990). Niflumic and flufenamic acids are potent reversible blockers of Ca-activated Cl channels in *Xenopus* oocytes. *Molecular Pharmacology* **37**, 720–724.

WONG, B. S. (1991). Ionic conductances in dissociated smooth muscle cells. *Proceedings of the Society for Experimental Biology and Medicine* **197**, 125–134.

YAMAMOTO, Y., HU, S. L. & KAO, C. Y. (1989). Inward current in single smooth muscle cells of the guinea pig taenia coli. *Journal of General Physiology* **93**, 521–550.